

Brain Network Analysis of Compressive Sensed High-Density EEG Signals in AD and MCI Subjects

Nadia Mammone^{ID}, Member, IEEE, Simona De Salvo, Lilla Bonanno^{ID}, Cosimo Ieracitano^{ID}, Silvia Marino, Angela Marra, Alessia Bramanti, and Francesco C. Morabito^{ID}, Senior Member, IEEE

Abstract—Alzheimer’s disease (AD) is a neurodegenerative disorder that causes a loss of connections between neurons. The goal of this paper is to construct a complex network model of the brain-electrical activity, using high-density EEG (HD-EEG) recordings, and to compare the network organization in AD, mild cognitive impaired (MCI), and healthy control (CNT) subjects. The HD-EEG of 16 AD, 16 MCI, and 12 CNT was recorded during an eye-closed resting state. The permutation disalignment index (PDI) was used to describe the dissimilarity between EEG signals and to construct the connection matrices of the network model. The three groups were found to have significantly different ($p < 0.001$) characteristic path length (λ), average clustering coefficient (CC), and the global efficiency (GE). This is the first time that HD-EEG signals of AD, MCI, and CNT have been compared and that PDI has been used to discriminate between the three groups. Considering the large amount of data originating from HD-EEG acquisition, compared to standard EEG, the aim of this paper is also to assess that compression did not alter the results of the complex network analysis. Compressive sensing was adopted to compress and reconstruct the HD-EEG signals with minimal information loss, achieving an average structural similarity index of 0.954 (AD), 0.957 (MCI), and 0.959 (CNT). When applied to the reconstructed HD-EEG, complex network analysis provided a substantially unaltered performance, compared to the analysis of the original signals: λ , CC, and GE of the three groups were indeed still significantly different ($p < 0.001$).

Index Terms—Alzheimer’s disease (AD), brain connectivity, compressive sensing (CS), decision support, healthcare

Manuscript received May 9, 2018; accepted August 20, 2018. Date of publication September 3, 2018; date of current version January 3, 2019. This work was funded by the Italian Ministry of Health, project code: GR-2011-02351397. Paper no. TII-18-1172. (Corresponding author: Lilla Bonanno.)

N. Mammone, S. De Salvo, L. Bonanno, S. Marino, and A. Marra are with the IRCCS Centro Neurolesi Bonino Pulejo, Messina 98124, Italy (e-mail: nadia.mammone@irccsme.it; simona.desalvo@irccsme.it; lilla.bonanno@irccsme.it; silvia.marino@irccsme.it; angela.marra@irccsme.it).

C. Ieracitano and F. C. Morabito are with the Department of Civil, Energy, Environmental and Materials Engineering, Mediterranean University of Reggio Calabria, Reggio Calabria 89060, Italy (e-mail: cosimo.ieracitano@unirc.it; morabito@unirc.it).

A. Bramanti is with the Institute of Applied Sciences and Intelligent Systems “Eduardo Caianiello,” National Research Council, Messina 98164, Italy (e-mail: alessia.bramanti@irccsme.it).

Color versions of one or more of the figures in this paper are available online at <http://ieeexplore.ieee.org>.

Digital Object Identifier 10.1109/TII.2018.2868431

signal processing, high-density EEG (HD-EEG), mild cognitive impairment, permutation disalignment index.

I. INTRODUCTION

THE incidence of dementia is gradually increasing due to aging world population [1]. Alzheimer’s disease (AD) is the most common form of dementia as it is estimated to account for 60% of all the dementia cases [1]. Experts postulated that AD arises with a subtle preclinical stage, develops through an intermediate amnesic mild cognitive impairment (MCI) stage, and ends up with a final dementia stage, when cognitive impairment affects the ability to live independently [2]. The early diagnosis of AD, which would dramatically improve patient’s treatment, would be possible only if the current diagnostic tools were improved. High-density EEG (HD-EEG) could make a significant contribution, thanks to its significantly higher spatial resolution than standard EEG. Two main features commonly characterize EEG signals recorded from AD patients, compared to elderly healthy controls (CNT): the so-called *slowing effect* (a reduction of the power at low frequencies together with an increase at high frequencies) and the reduction of synchrony between pairs of EEG signals [3]. Such effects seem to be caused by disrupted segregation and integration in brain networks due to the functional disconnection caused by neuronal death [4]. Such a functional disconnection phenomenon seems to reflect upon the efficiency of brain-electrical connectivity, as shown by Frantidis *et al.* [5] who investigated functional connectivity in mild AD and MCI, through the relative wavelet entropy of EEG signals, and reported a weakened functional network organization in both groups. Morabito *et al.* [6] detected a decline in the functional connectivity of AD patients that were evaluated longitudinally. Vecchio *et al.* [7] found that a larger hippocampal volume was associated with lower alpha and higher delta, beta, and gamma small worldness in AD patients, compared to CNT. Tahaei *et al.* reported a decreased synchronizability of brain networks across delta, alpha, beta, and gamma EEG frequency bands [8]. De Haan *et al.* [9] observed that large-scale functional brain network organization in AD patients seems to degenerate from the optimal small-world behavior toward a more random one. Permutation disalignment index (PDI) was recently introduced as a descriptor of dissimilarity between time series [10]. A PDI-based complex network analysis was recently proposed to

detect longitudinal changes in the brain-electrical network organization of MCI subjects, estimated from 19-channels standard EEG, network organization deterioration resulted positively correlated to cognitive decline [11].

One of the main advantages of EEG is the very good temporal resolution; however, the spatial resolution of standard EEG is poor, either because of volume conduction effects and because of the large interelectrode distance [12]. Ryynanen *et al.* reported that some information of the scalp electrical potentials is lost unless an intersensor distance of 1–2 cm is used [13]. With standard 10–20 EEG systems, the average intersensor distance is 7 cm, and with 256-channels HD-EEG, a very good approximate spatial resolution is achieved [13]. The potential of HD-EEG has been widely proven in other fields, like in the identification of the epileptic onset zone through electrical source imaging [14], whereas there are just a few studies based on HD-EEG in the literature on AD. In particular, Aghajani *et al.* [15] applied standardized low-resolution brain electromagnetic tomography to compare eye-closed resting state HD-EEGs recorded from AD patients and CNT and found that the right brain hemisphere of AD subjects showed a reduced activity in all frequency bands. Dubovik *et al.* [16] investigated modifications in functional connectivity of resting state 128-channels HD-EEGs recorded from AD and elderly CNT. They observed that medial temporal and parietal lobes of AD patients resulted disrupted in alpha band; however, an adaptive reorganization of the language network was also observed to the right hemisphere. In summary, the potential of HD-EEG in the dementia field is still largely unexplored. This paper proposes the use of a complex network approach, based on PDI between pairs of HD-EEG signals, to compare the brain network organization of AD, MCI, and CNT. Three cohorts of 16 AD patients, 16 MCI subjects, and 12 CNT were enrolled on purpose at IRCCS Centro Neurolesi Bonino Pulejo (Messina, Italy). This is the first time that resting-state HD-EEG signals of AD, MCI, and CNT have been compared and that PDI has been used to identify cross-sectional differences between the three groups. HD-EEG offers a high temporal resolution, typical of standard EEG recordings, together with a significantly increased spatial resolution, which means that a large amount of data are recorded, compared to standard low-density EEG. This may cause issues in sharing data within multicentric studies or in telemonitoring applications, which will be engaged in the near future at IRCCS Centro Neurolesi Bonino Pulejo. The size of the dataset needs, therefore, to be optimized and the integrity of the diagnostic features after compression needs to be assessed. To this purpose, the compressive sensing (CS) block sparse Bayesian learning (BSBL) approach [17] was adopted to compress and subsequently reconstruct the HD-EEG signals. The proposed PDI-based complex network analysis was then applied to the reconstructed HD-EEGs in order to assess that compression did not alter the estimation of the features of brain-network organization. This paper is organized as follows. Section II illustrates how patients were enrolled and how their HD-EEGs were acquired and preprocessed. Section III describes the proposed PDI-based complex network approach and the application of CS to the HD-EEG dataset. Section IV

reports the results, Section V discusses the achieved results, and Section VI infers some conclusions.

II. MATERIALS: HD-EEG DATASET

A. Patients' Description

Three groups of subjects were recruited at IRCCS Centro Neurolesi Bonino Pulejo: 16 AD patients (9 female, age 74 ± 10), 16 amnesic MCI subjects (11 female, age 69 ± 8), and 12 elderly CNT (7 female, age 62 ± 4). All the medical evaluations and examinations were conducted by a team of neurologists, neuropsychologists, and EEG experts. The study followed a clinical protocol approved by the local ethics committee. The inclusion criteria were the diagnosis of MCI or AD, according to the *Diagnostic and Statistical Manual of Mental Disorders* (5th ed.) [18]. The exclusion criteria were: evidence of other neurological or psychiatric disorders that may cause cognitive impairment; complex or uncontrolled systemic disorders; traumatic brain injury; EEG epileptiform activity; and treatment with any psychoactive medication. The subjects were informed about the goals, the risks, and the benefits of the study, as well as about the steps of the procedure. The patients and their caregivers signed an informed consent form that reported all the aforementioned information. Every subject was examined neuroradiologically, in order to exclude any other possible pathological condition like traumatic brain injury, stroke, hydrocephalus, or any other neurological condition.

B. HD-EEG Recording and Preprocessing

EEG signals were acquired by means of a high-density 256-channels *EGI Sensor Net*, that is part of the *Electrical Geodesics EEG system* [see Fig. 1(b)]. The reference electrode was set as the central sensor (Cz) and the sampling rate was set at 250 Hz. Every channel x records the differential potential between its own electrode location x and the reference location. As suggested by the EGI guidelines, electrode impedances were kept lower than 50 k Ω . The EEGs were acquired in the morning. Before the recording session started, every patient and her/his caregivers were interviewed about the last meal and about the quality and length of the last night sleep. The subjects kept their eyes closed but remained awake during the recording; the physician visually checked the EEG traces in real time in order to promptly detect any possible pattern of drowsiness. The EEG signals were bandpass filtered between 1 and 40 Hz by means of the *Net Station EEG software* (which is part of the *Electrical Geodesics EEG system*) in order to capture the major neurological subbands: delta (1–4 Hz), theta (4–8 Hz), alpha (8–13 Hz), beta (13–30 Hz), gamma (>30 Hz). The filtered recordings were later manually reviewed by the EEG experts and the artifactual segments were detected and canceled. In all, 2 min of artifact-free resting state HD-EEG were finally selected for each patient. In total, 173 out of the 256 available channels were included in the analysis, excluding the electrodes corresponding to the cheeks and the neck, as they are contaminated by muscle artifacts and are not relevant to the study of

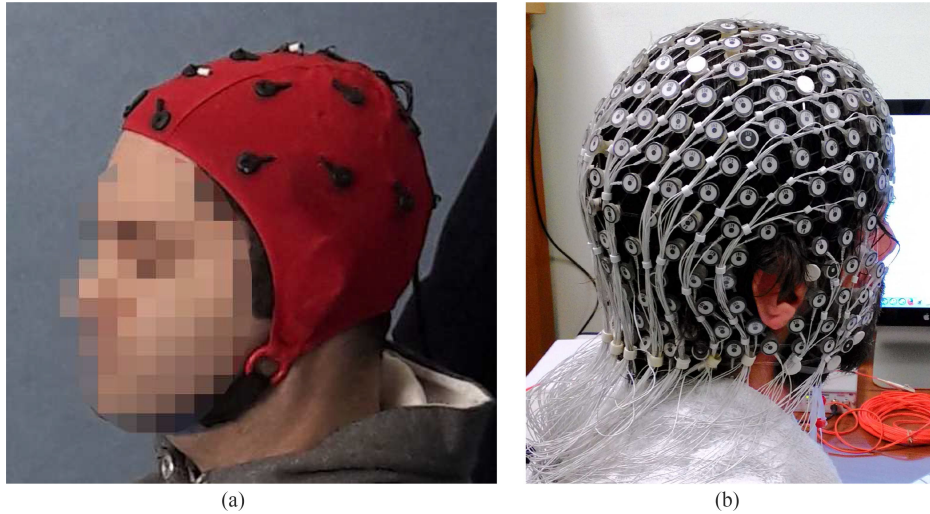


Fig. 1. EEG recording system. (a) Standard 19-channels EEG. (b) High-density 256-channels *Electrical Geodesics EEG* system used in this paper.

the electrical activity of the cortex. The preprocessed HD-EEG signals were exported as a MATLAB *.mat* file and then fed into the PDI-based complex network analysis algorithm, which was fully implemented in MATLAB 2016a (The MathWorks, Inc., Natick, MA, USA).

III. METHODOLOGY: COMPLEX NETWORK MODEL BASED ON PDI BETWEEN EEG SIGNALS

The first objective of this paper is to explore the potential of HD-EEG-based complex network analysis to capture differences in the brain-electrical network organization of AD, MCI, and CNT subjects. To this purpose, it was necessary to adopt a graph representation of the interaction between the electrical activity of the different areas of the cortex. The cortical areas are uniformly covered by the electrodes of the sensor net [see Fig. 1(b)], which represent the *nodes* of the network. The weight of an *edge* connecting two nodes (electrodes) is determined by estimating the *coupling strength* between the two corresponding EEG signals. In this way, a graph representation of the brain-electrical network interaction is constructed. Such a graph model is estimated for every subject (i.e., every HD-EEG recording) and its quantitative analysis indirectly provides information about the efficiency of the brain-electrical network organization in that subject. Every HD-EEG recording was segmented into nonoverlapping epochs of 1 s and it was processed epoch by epoch. Thus, for each subject, 120 epochs were analyzed. In total, $120 \times 16 = 1920$ epochs of AD patients, 1920 epochs of MCI subjects, and $120 \times 12 = 1440$ epochs of CNT were included in the analysis. As regards the choice of the coupling strength descriptor, PDI was recently proposed as a measure of dissimilarity, it is inversely proportional to the coupling strength between time series [10], and it was successfully applied to standard 19-channels EEGs of AD and MCI patients [11]. Section VI will briefly recall how PDI is calculated. For every epoch “*e*,” the $\text{PDI}^e(x, y)$ between every possible pair of electrodes *x* and *y* was calculated. Since $n = 173$ is the number

of electrodes, there are $n(n - 1)/2 = 14\,878$ possible pairs of channels. $\text{PDI}^e(x, y)$ is the (x, y) th element of the dissimilarity matrix \mathbf{PDI}^e of epoch *e*. Since $\text{PDI}^e(x, y) = \text{PDI}^e(y, x)$, \mathbf{PDI}^e matrix is symmetrical and the graph model is therefore undirected. Once the analysis of the entire HD-EEG recording of a subject is completed, the sequence of matrices \mathbf{PDI}^e is determined for every epoch (with $e = 1, \dots, 120$). The whole sequence is then normalized by dividing by the maximum value of the entire sequence so that the elements of the matrices \mathbf{PDI}^e fall in the range 0–1.

A. Weighted Complex Network Analysis

The first goal was to evaluate the efficiency of the complex network organization, as it reflects the efficiency of the underlying cortical-electrical network organization. Network efficiency was evaluated for every HD-EEG of the dataset and every epoch *e*. The *characteristic path length* (λ), the *average clustering coefficient* (CC), and the *global efficiency* (GE) [19] were calculated for every dissimilarity matrix \mathbf{PDI}^e . The characteristic path length (λ) measures the global integration within a network [19]. It is defined as

$$\lambda = \frac{1}{n(n-1)} \sum_{\substack{i \neq j \\ i, j \in V}} d_{i,j}$$

where $d_{i,j}$ is the shortest distance between node *i* and *j*. The distance between two nodes *i* and *j*, in a weighted network, is the sum of the weights of the edges that will be traversed to get from *i* to *j*. In this paper, the weight of the edge connecting *i* and *j* is equal to $\text{PDI}^e(i, j)$.

The GE is the average inverse shortest path length ($d_{i,j}$) [19] and is defined as

$$\text{GE} = \frac{1}{n} \sum_{i \in V} \frac{\sum_{j \in V, j \neq i} (d_{i,j})^{-1}}{n-1}.$$

The higher the GE, the higher the overall transmission efficiency within a network.

The CC is a measure of segregation and quantifies the possibility that two neighbors of node i become neighbors of each other. The average CC is defined as

$$CC = \frac{1}{n} \sum_{i=1}^n CC_i = \frac{1}{n} \sum_{i \in V} \frac{2t_i}{k_i(k_i - 1)}$$

where CC_i represents the CC of node i . It is determined by t_i , the number of the connections around node i , and by the maximum number of possible connections of that node, which can be calculated as $k_i(k_i - 1)/2$, where k_i is the degree of node i [19]. The degree of a node, in a weighted network, is the sum of the weights of the edges connected to that node. In order to avoid to misinterpret the results of the complex network analysis, a surrogate analysis approach was adopted to normalize the estimated parameters with respect to those obtained from random networks [20]. Since the adopted PDI-based complex network model is consisted in a fully connected weighted graph with 173 nodes, the network size is stable over the epochs and over the subjects. For every subject, 120 dissimilarity matrices are estimated, with $e = 1, \dots, 120$. For every dissimilarity matrix \mathbf{PDI}^e , 4096 surrogate matrices \mathbf{PDI}_s^e are generated by reshuffling the weights randomly [20]. The parameters λ_s , CC_s , GE_s of the 4096 surrogate matrices \mathbf{PDI}_s^e are calculated and then averaged. The parameters estimated from the original network \mathbf{PDI}^e are finally normalized by the average surrogate parameters: $\lambda_n = \lambda/\lambda_s$, $CC_n = CC/CC_s$, and $GE_n = GE/GE_s$.

B. Connectivity Density Analysis

For every HD-EEG (i.e., subject) and every epoch e , a *connectivity density* analysis was also carried out by analyzing the dissimilarity matrix \mathbf{PDI}^e of that epoch. Given a \mathbf{PDI}^e , the complementary *connection matrix* $\mathbf{CM}^e = 1 - \mathbf{PDI}^e$ is calculated. The \mathbf{CM}^e matrix is then binarized through a threshold th (ranging from 0 to 1 with a 0.1 step) by setting the connection $\mathbf{CM}^e(i, j)$ to 0 if $\mathbf{PDI}^e(i, j) > th$ or to 1 if $\mathbf{PDI}^e(i, j) \leq th$. Channels i and j are indeed considered “connected” if $\mathbf{PDI}^e(i, j) \leq th$ because PDI is a measure of dissimilarity. Given a threshold th , the number of active connections in the network $Nac(th)$ is counted and the related network density $ND^e(th)$ is calculated as

$$ND^e(th) = \frac{Nac(th)}{Npc(th)}$$

where $Npc(th)$ is the overall number of possible connections in the network (calculated as $n(n - 1)/2 = 173 * (173 - 1)/2 = 14\,878$). Finally, given a subject, an epoch e and a threshold th , $ND^e(th)$ is averaged over the epochs so that an overall $\overline{ND}(th)$ of that subject is estimated for the threshold th under consideration.

C. CS of EEG Signals

CS is a signal processing technique that is able to recover the original data even from a smaller number of samples than conventional approaches. CS is based on the assumption that

most of natural signals have sparse or compressible properties. Let $\mathbf{x} \in R^{N \times 1}$ be a signal and let K ($K \ll N$) be the nonzero coefficients of \mathbf{x} ; then, the vector \mathbf{x} is denoted as K - sparse. This means that a lot of entries ($N - K$) of \mathbf{x} are zero. However, a signal $\mathbf{x} = [x_1, x_2, \dots, x_N]$ can show sparsity when expressed in suitable orthonormal basis $\Psi = [\psi_1, \psi_2, \dots, \psi_N]$

$$\mathbf{x} = \Psi \mathbf{s} \quad (1)$$

where $\mathbf{s} = [s_1, s_2, \dots, s_N]$ is the sparse transform domain vector.

The typical formulation of the compressed sensing problem is

$$\mathbf{y} = \Phi \mathbf{x} \quad (2)$$

where \mathbf{y} denotes the compressed representation (sized M with $M < N$), \mathbf{x} is the sparse signal, and Φ is the so-called *measurement matrix*. Thus, the signal \mathbf{x} is projected onto the measurement matrix Φ , sized $M * N$. Applying the sparse transform representation (1), the previous formulation can be rewritten as

$$\mathbf{y} = \Phi \Psi \mathbf{s} = \mathbf{C} \mathbf{s} \quad (3)$$

where \mathbf{C} is the so-called *sensing matrix*. The CS procedure first recovers \mathbf{s} from \mathbf{y} and $\Phi \Psi$; and then, reconstructs the original \mathbf{x} by using (1). Further details on CS can be found in [21]. Although CS is a promising technique, it can be applied only to a few physiological signals. In this regard, the EEG recording is not a sparse signal neither in the time nor in the transformed domain, but this issue was overcome by Zhang and Rao [22] by applying BSBL, which was adopted in this paper. Through the BSBL framework, EEG signals can be recovered by adopting the compressed sensing formulation (3). For example, in telemonitoring applications, the original HD-EEG (\mathbf{x}) can be compressed (\mathbf{y}) and transferred to a remote user. HD-EEG signals are then reconstructed by the user according to (3); the CS algorithm indeed knows matrix Φ for recovery [17]. The recovery quality may be measured by mean square error (MSE) and structural similarity index (SSIM) [17]. SSIM is a better recovery performance parameter than MSE; it estimates the similarity between the original and the reconstructed signal. High values of SSIM indicate good recovery quality. SSIM = 1 means perfect reconstruction of the original signal.

IV. RESULTS

A. Complex Network Analysis of Original HD-EEG

Given an HD-EEG recording (i.e., a subject) and an epoch e (for every subject, there are 120 epochs of 1 s each), a dissimilarity matrix \mathbf{PDI}^e is determined according to Section III. The graph analysis described in Section III is carried out and the network parameters λ , average CC, and GE are calculated. Consider, for example, the λ parameter, three vectors (populations) are constructed (Lambda-AD, Lambda-MCI, and Lambda-CNT), each one containing the λ values calculated for all the epochs of the related group. Lambda-AD and Lambda-MCI are vectors with 1920 ($= 16 * 120$) elements, whereas Lambda-CNT is sized 1440 ($= 12 * 120$). Vectors CC-AD, CC-MCI, CC-CNT, GE-AD, GE-MCI, and GE-CNT are constructed in the same way. Fig. 2(a) shows the boxplots

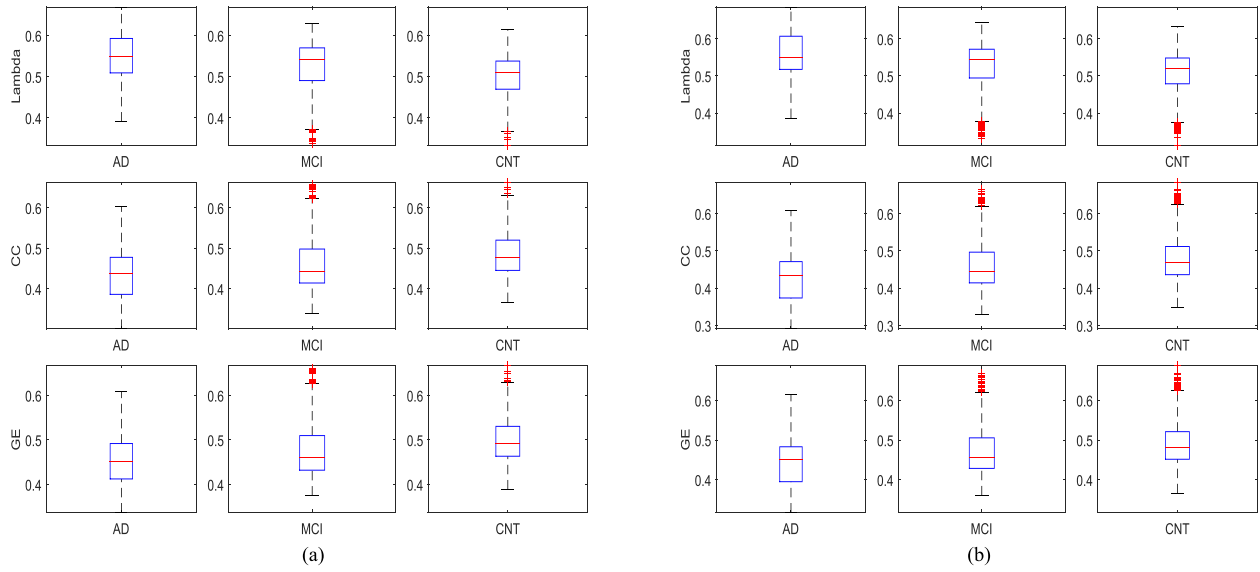


Fig. 2. Boxplot of the parameters λ , CC, and GE estimated by the PDI-based complex network analysis of the HD-EEGs of the three groups of subjects: AD, MCI, and CNT. The horizontal mark within each box represents the median, the edges of the box represent the first and third quartile, and the whiskers extend to the most extreme data points that are not considered outliers. (a) Complex network analysis of the original EEG. (b) Complex network analysis of the compressed and reconstructed EEG.

of the λ , CC, and GE vectors for all the three groups. A difference between the three groups can be observed and, in order to validate this observation statistically, a comparison was carried out by means of the Mann–Whitney U test [23]. The analyses were performed using an open-source R3.0 software package (R Foundation for Statistical Computer, Vienna, Austria). A 95% confidence level was selected with a 5% alpha error; therefore, the statistical significance was set at $p < 0.05$. The results of the statistical analysis are reported in Table I (column “HD-EEG”). The numerical data are presented in terms of median and of first–third (I–III) quartile because the populations were estimated to have no normal distribution by means of the Shapiro–Wilk test [24]. The network parameters (λ , CC, GE) of the three groups resulted significantly different from each other ($p < 0.001$). In particular, the AD group was found to have a higher median λ , a lower median CC, and a lower median GE than the MCI group which, in turn, showed the same behavior with respect to the CNT group.

In order to compare PDI with other well-known descriptors of coupling strength, the proposed complex network analysis was carried also by replacing PDI with the phase lag index (PLI), a measure of asymmetry of the phase difference distribution between two time series [25]. In this case, MCI group exhibited significantly different network parameters ($p < 0.001$) from either AD and CNT, whereas the comparison AD versus CNT did not exhibit any significant difference (λ : $p = 0.46$; CC: $p = 0.59$; and GE: $p = 0.18$). Thus, PDI outperformed PLI in eliciting cross-sectional differences between the EEG-based complex network parameters of AD, MCI, and elderly controls. For every subject and every epoch e , the connectivity density analysis described in Section III-B was also carried out by analyzing the dissimilarity matrix \mathbf{PDI}^e of that epoch. Fig. 4(a) shows the mean ND versus th for the group of AD, MCI, and CNT subjects. Globally, the ND of the AD group resulted lower

TABLE I
OBTAINED RESULTS BY VISUAL INSPECTION AND MAXIMUM POWER DETERMINATION

HD-EEG				compressed HD-EEG			
	Median	I-III	p		Median	I-III	p
Lambda AD	0,550	0,518-0,607	<0,001	Lambda AD	0,55	0,518-0,607	<0,001
Lambda MCI	0,545	0,495-0,572		Lambda MCI	0,545	0,495-0,572	
Lambda AD	0,550	0,518-0,607	<0,001	Lambda AD	0,55	0,518-0,607	<0,001
Lambda CNT	0,519	0,479-0,549		Lambda CNT	0,519	0,479-0,549	
Lambda MCI	0,545	0,495-0,572	<0,001	Lambda MCI	0,545	0,495-0,572	<0,001
Lambda CNT	0,519	0,479-0,549		Lambda CNT	0,519	0,479-0,549	
	Median	I-III	p		Median	I-III	p
CC AD	0,434	0,374-0,471	<0,001	CC AD	0,4340	0,374-0,471	<0,001
CC MCI	0,444	0,414-0,497		CC MCI	0,444	0,414-0,197	
CC AD	0,434	0,374-0,471	<0,001	CC AD	0,4340	0,374-0,471	<0,001
CC CNT	0,468	0,436-0,512		CC CNT	0,468	0,436-0,512	
CC MCI	0,444	0,414-0,497	<0,001	CC MCI	0,444	0,414-0,197	<0,001
CC CNT	0,468	0,436-0,512		CC CNT	0,468	0,436-0,512	
	Median	I-III	p		Median	I-III	p
GE AD	0,4520	0,412-0,492	<0,001	GE AD	0,452	0,395-0,483	<0,001
GE CNT	0,491	0,463-0,530		GE CNT	0,481	0,452-0,521	
GE AD	0,4520	0,412-0,492	<0,001	GE AD	0,452	0,395-0,483	<0,001
GE MCI	0,460	0,432-0,51		GE MCI	0,456	0,429-0,525	
GE MCI	0,460	0,432-0,51	<0,001	GE MCI	0,456	0,429-0,525	<0,001
GE CNT	0,491	0,463-0,530		GE CNT	0,481	0,452-0,521	

than the MCI group which, in turn, showed a lower ND than the CNT group. This result corroborates the hypothesis that AD is a phenomenon of neuronal disconnection [6] and that amnesic MCI can be an intermediate condition between AD and normal aging [26].

B. Complex Network Analysis of Compressively Sensed HD-EEG

The next step was to pass the HD-EEGs through CS to assess if the PDI-based complex network analysis, when carried out on the compressed and then reconstructed HD-EEG, was still able to highlight differences between the three groups. The HD-EEGs were processed as described in Section III-C; in particular, bi-

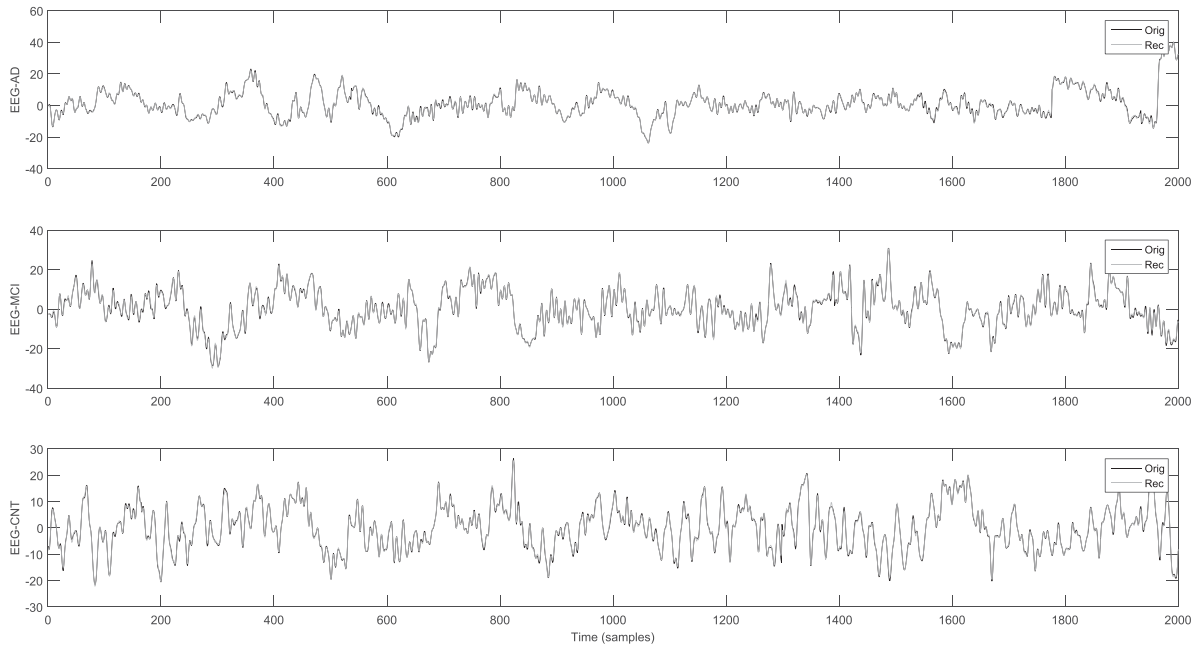


Fig. 3. Three original EEG signals (black) and the related compressive sensed and reconstructed signals (gray): for an AD patient, an MCI, and a CNT subject.

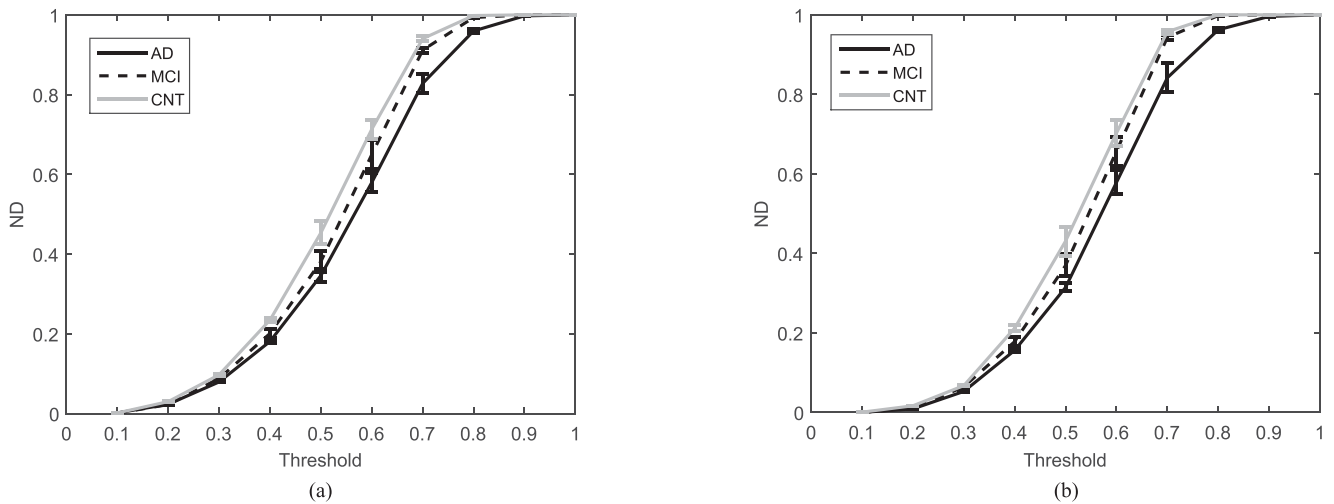


Fig. 4. Network density estimated by the PDI-based complex network analysis of the HD-EEGs of the three groups of subjects: AD, MCI, and CNT. ND was estimated by binarizing the weighted connection matrix for different threshold values, as detailed in Section III-B. (a) ND estimated from the original HD-EEG. (b) ND estimated from the compressed and reconstructed HD-EEG.

nary sparse Φ matrices of size 192×384 were used [17]. Given a generic HD-EEG recorded from one of the subjects under examination, it is stored as an $n \times N_s$ matrix, where $n = 173$ and, if f_s is the sampling rate, $N_s = 120 \times f_s = 120 \times 250 = 30000$ is the number of samples. This matrix is then processed channel by channel, by dividing the single HD-EEG signal into nonoverlapping windows with 384 elements each [17]. **Fig. 3** shows three original EEG signals (AD, MCI, and CNT) and the related reconstructed signals. The reconstruction is good in all the three cases, and the gray signals indeed almost perfectly overlap to the original ones. The quality of the reconstruction was evaluated by SSIM and MSE [17]. SSIM and MSE were

estimated for every subject, every epoch, and every channel, and then they were averaged over the epochs, over the channels, and over the subjects of each group. The following values were obtained: average MSE 0.008 (AD), 0.006 (MCI), 0.006 (CNT); average SSIM 0.954 (AD), 0.957 (MCI), 0.959 (CNT). In order to assess that compression did not affect the estimation of complex network features, the PDI-based graph analysis described in Section III was applied also to the HD-EEG dataset reconstructed after compression. **Fig. 2(b)** shows the boxplots of the network parameters of the three groups AD, MCI, and CNT calculated from the compressed and then reconstructed EEG signals. Also when analyzing the reconstructed HD-EEG,

a difference between the three groups could be observed. The statistical analysis described in Section IV-A was adopted to validate this result. In particular, as reported in Table I (“compressed HD-EEG” column), the AD group was again found to have higher median λ and lower median CC and GE than the MCI group ($p < 0.001$) and the MCI group showed the same behavior over the control group ($p < 0.001$). As regards the connectivity density analysis described in Section III-B, Fig. 4(b) shows the average ND versus th of the three groups. ND exhibited the same behavior as the original HD-EEG signals; thus, compression did not affect the ability of HD-EEG signals to describe the brain-electrical network organization.

V. DISCUSSION

Dementia is a problem that is gradually worsening in today’s society, due to the progressive increase in the average age of the world population [1]. Early diagnosis would improve the treatment protocols of patients with AD, but it would be possible only if the current diagnostic means were improved. HD-EEG could make a significant contribution in this field as it is a fast and relatively cheap methodology (compared to other methods such as magnetic resonance imaging or magnetoencephalography) that is well tolerated also by dementia patients. The potential of HD-EEG has already been demonstrated in the study of neurological diseases such as epilepsy [14] but it is still largely unexplored in the dementia field. In the literature, AD was shown to be characterized by a worsening in the brain network organization due to a reduced connectivity caused by the deposit of plaques and by neuronal death [27]. Some works in the literature studied the brain network organization in AD patients by applying complex network methods to EEG signals [5], [7]. Recently, PDI was introduced as a new parameter to describe the dissimilarity between time series [10] and was successfully applied to the longitudinal study of standard low-density EEG recorded from MCI subjects [11]. This paper presents a PDI-based complex network analysis conducted on HD-EEGs recorded from 16 AD patients, 16 MCI subjects, and 12 CNT. This is the first time that resting-state HD-EEG signals of AD, MCI, and elderly CNT subjects have been studied and that PDI has been used to identify cross-sectional differences between the three groups. The proposed PDI-based complex network analysis provided significantly different network parameters (λ , CC, GE) for the three groups ($p < 0.001$). In particular, AD group was found to have higher median λ and lower median CC and GE than the MCI group and, in turn, the MCI group exhibited the same behavior with respect to the control group. This endorses the hypothesis that AD evolves together with a progressive reduction of the network organization efficiency [5] and that MCI holds intermediate characteristics between AD and healthy aging. Since electroencephalographic signals have a high temporal resolution, by increasing the spatial resolution with HD-EEG (standard EEG normally includes 19 channels, whereas HD-EEG can include even 256 channels), a lot of more detailed information about the brain-electrical activity are collected, which unavoidably produces a very large amount of data. EEG signals are often meant to be shared with other centers and will be

used in the near future in telemonitoring applications at IRCCS Centro Neurolesi Bonino Pulejo. This makes strictly necessary to optimize the dataset size and to assess the integrity of the diagnostic features extracted from the compressed and then reconstructed data. In this paper, the BSBL approach proposed by Zhang *et al.* [17] was adopted to compress and subsequently reconstruct the HD-EEG signals, obtaining a reconstruction with minimal information loss [average MSE: 0.008 (AD), 0.006 (MCI), 0.006 (CNT); average SSIM: 0.954 (AD), 0.957 (MCI), 0.959 (CNT)]. The PDI-based complex network analysis was then applied also to the reconstructed HD-EEG signals, showing substantially unaltered performance, compared to the analysis of the original signals. Although the proposed analysis allowed to unveil differences between the AD, MCI, and CNT groups, an intersubject variability of the network characteristics within the same group was observed. Furthermore, by analyzing the network characteristics of the 120 epochs of every subject, it could be observed that epochs belonging to the same subject exhibited similar network parameters, which means that the subjects exhibited stable network parameters during the resting state recording. This observation suggests that intrasubject longitudinal differences could be even more significant than the intersubject cross-sectional ones. The intrasubject longitudinal analysis could allow to find out how the pathology affects the individual’s brain network organization over the time and in what extent these effects are related to cognitive decline. The future objective will be to recruit a significant number of AD and MCI subjects, to be monitored longitudinally through HD-EEG, in order to investigate in detail spatial-temporal changes in the brain-electrical connectivity of every single patient. Recently, NeuCube, an evolving spatio-temporal data machine, was successfully applied to evaluate longitudinal changes in the EEG recording of AD patients [28], [29]. Those studies showed how NeuCube system can be used to analyze AD EEG data collected longitudinally. By means of the proposed model, patterns of longitudinal changes in neurons’ electrical activity were investigated. In the future, NeuCube could be complemented with the proposed PDI-based methodology in order to provide a deep insight into the brain-electrical connectivity deterioration caused by AD.

VI. CONCLUSION

In this paper, a cross-sectional complex network study was carried out to compare the characteristics of the brain network organization in AD, MCI, and healthy elderly subjects by analyzing their HD-EEG recordings. A cohort of 16 AD, 16 MCI, and 12 CNT was recruited and their HD-EEG signals were recorded during a comfortable eye-closed resting state. The PDI was used to describe the dissimilarity between EEG signals and to subsequently build the connectivity matrices that the complex network model was based on. The proposed PDI-based complex network analysis revealed that the network parameters (λ , CC, GE) of the three groups were significantly different ($p < 0.001$). In particular, AD group exhibited higher median λ and lower median CC and GE than the MCI group, which, in turn, exhibited the same behavior with respect to CNT group.

This result endorses the hypothesis that AD involves a progressive reduction of the network organization's efficiency and that amnesic MCI subjects exhibit intermediate characteristics between AD and healthy elderly controls. Furthermore, given the inherent and not trivial issue of the large amount of data originating from HD-EEG acquisition, the issue of EEG compression was also addressed in this paper. The BSBL approach [17] was adopted to compress and subsequently reconstruct the HD-EEG signals, obtaining a reconstruction with minimal information loss, in particular, average MSE: 0.008 (AD), 0.006 (MCI), 0.006 (CNT); average SSIM: 0.954 (AD), 0.957 (MCI), 0.959 (CNT). When applied to the reconstructed HD-EEG, the PDI-based complex network analysis provided a substantially unaltered performance, compared to the analysis of the original signals. The parameters λ , CC, GE of the three groups were indeed still significantly different ($p < 0.001$). HD-EEG compression did not alter the complex network analysis and could be applied in future telemonitoring applications where EEG is meant to be remotely processed.

APPENDIX

PERMUTATION DISALIGNMENT INDEX

PDI was first defined in [10] and is described in detail in that paper. It was inspired by the concept of time series projection into symbols (*motifs*) proposed by Bandt and Pompe for permutation entropy (PE) [30]. PE is a univariate descriptor that quantifies the randomness of one time series at a time. PDI is a multivariate descriptor of the coupling strength between two or more time series. It measures the randomness of the disalignment between motifs derived from the signals by projecting equally spaced samples into the m -dimensional embedding space. The distance between one selected sample and the next one is equal to L , which is known as *time lag*, whereas m is named *embedding dimension* [30]. Given two signals x_i and x_j , recorded at two EEG electrode locations i and j , PDI estimates the entropy (according to Renyi's definition [10]) of the simultaneous occurrence of every possible motif π_k (with $k = 1, \dots, m!$) in both x_i and x_j . PDI between x_i and x_j is defined as

$$\text{PDI}(x_i, x_j) = \frac{1}{1 - \alpha} \log \left[\sum_{k=1}^{m!} p_{x_i, x_j}(\pi_k)^\alpha \right] \quad (4)$$

where $p_{x_i, x_j}(\pi_k)$ is the probability that a given motif π_k simultaneously occurs in x_i and x_j and α is the order of entropy according to Renyi's theory [10]. $\text{PDI}(x_i, x_j)$ is inversely proportional to the coupling strength between x_i and x_j ; coupled signals are indeed expected to exhibit the same motifs with increased probability [10]. In this paper, $m = 3$ and $L = 1$ are the values selected for the embedding dimension and the time lag [10]. The entropy order α modulates the sensitivity to the Gaussianity of the probability density function distribution of the signals: $\alpha \leq 2$ emphasizes sub-Gaussianity, whereas $\alpha \geq 2$ emphasizes super-Gaussianity. Average *alpha* values ($\alpha \simeq 2$) equally emphasize both and were adopted in this paper.

REFERENCES

- [1] M. Prince, A. Comas-Herrera, M. Knapp, M. Guerchet, and M. Karagianidou, "World Alzheimer Report 2016: Improving healthcare for people living with dementia: Coverage, quality and costs now and in the future," *Alzheimer's Dis. Int.*, London, U.K., 2016. [Online]. Available: <http://eprints.lse.ac.uk/67858/>
- [2] R. A. Sperling *et al.*, "Toward defining the preclinical stages of Alzheimer's disease: Recommendations from the National Institute on Aging-Alzheimer's Association workgroups on diagnostic guidelines for Alzheimer's disease," *Alzheimer's Dementia*, vol. 7, no. 3, pp. 280–292, 2011.
- [3] H. Adeli, S. Ghosh-Dastidar, and N. Dadmehr, "Alzheimer's disease: Models of computation and analysis of EEGs," *Clin. EEG Neurosci.*, vol. 36, no. 3, pp. 131–140, 2005.
- [4] H. Adeli, S. Ghosh-Dastidar, and N. Dadmehr, "Alzheimer's disease and models of computation: Imaging, classification, and neural models," *J. Alzheimer's Dis.*, vol. 7, no. 3, pp. 187–199, 2005.
- [5] C. A. Frantzidis, A. B. Vivas, A. Tsolaki, M. A. Klados, M. Tsolaki, and P. D. Bamidis, "Functional disorganization of small-world brain networks in mild Alzheimer's Disease and amnesic mild cognitive impairment: An EEG study using relative wavelet entropy (RWE)," *Front Aging Neurosci.*, vol. 6, pp. 1–11, 2014.
- [6] F. C. Morabito *et al.*, "A longitudinal EEG study of Alzheimer's disease progression based on a complex network approach," *Int. J. Neural Syst.*, vol. 25, no. 2, 2015, Art. no. 1550005.
- [7] F. Vecchio *et al.*, "'Small World' architecture in brain connectivity and hippocampal volume in Alzheimer's disease: A study via graph theory from EEG data," *Brain Imag. Behav.*, vol. 11, no. 2, pp. 473–485, 2017.
- [8] M. S. Tahaei, M. Jalili, and M. G. Knyazeva, "Synchronizability of EEG-based functional networks in early Alzheimer's disease," *IEEE Trans. Neural Syst. Rehabil. Eng.*, vol. 20, no. 5, pp. 636–641, Sep. 2012.
- [9] W. De Haan *et al.*, "Functional neural network analysis in frontotemporal dementia and Alzheimer's disease using EEG and graph theory," *BMC Neurosci.*, vol. 10, no. 1, 2009, Art. no. 101.
- [10] N. Mammone *et al.*, "Permutation disalignment index as an indirect, EEG-based, measure of brain connectivity in MCI and AD patients," *Int. J. Neural Syst.*, vol. 27, 2017, Art. no. 1750020, doi: 10.1142/S0129065717500204.
- [11] N. Mammone *et al.*, "A permutation disalignment index-based complex network approach to evaluate longitudinal changes in brain-electrical connectivity," *Entropy*, vol. 19, no. 10, pp. 1–15, 2017.
- [12] P. L. Nunez and R. Srinivasan, *Electric Fields of the Brain: The Neurophysics of EEG*. New York, NY, USA: Oxford Univ. Press, 2006.
- [13] O. R. M. Ryyanen, J. A. K. Hyttinen, and J. A. Malmivuo, "Effect of measurement noise and electrode density on the spatial resolution of cortical potential distribution with different resistivity values for the skull," *IEEE Trans. Biomed. Eng.*, vol. 53, no. 9, pp. 1851–1858, Sep. 2006.
- [14] P. Mégevand *et al.*, "Electric source imaging of interictal activity accurately localises the seizure onset zone," *J. Neurol. Neurosurg. Psychiatry*, vol. 85, no. 1, pp. 38–43, 2014.
- [15] H. Aghajani, E. Zahedi, M. Jalili, A. Keikhosravi, and B. V. Vahdat, "Diagnosis of early Alzheimer's disease based on EEG source localization and a standardized realistic head model," *IEEE J. Biomed. Health Inform.*, vol. 17, no. 6, pp. 1039–1045, Nov. 2013.
- [16] S. Dubovik, A. Bouzerda-Wahlen, L. Nahum, G. Gold, A. Schnider, and A. G. Guggisberg, "Adaptive reorganization of cortical networks in Alzheimer's disease," *Clin. Neurophysiol.*, vol. 124, no. 1, pp. 35–43, 2013.
- [17] Z. Zhang, T.-P. Jung, S. Makeig, and B. D. Rao, "Compressed sensing of EEG for wireless telemonitoring with low energy consumption and inexpensive hardware," *IEEE Trans. Biomed. Eng.*, vol. 60, no. 1, pp. 221–224, Jan. 2013.
- [18] American Psychiatric Association, *Diagnostic and Statistical Manual of Mental Disorders*, 5th ed. Lake St. Louis, MO, USA: Amer. Psychiatric Publ., 2013.
- [19] A. Fornito, A. Zalesky, and E. Bullmore, *Fundamentals of Brain Network Analysis*. New York, NY, USA: Academic, 2016.
- [20] G. Ansmann and K. Lehnertz, "Surrogate-assisted analysis of weighted functional brain networks," *J. Neurosci. Methods*, vol. 208, no. 2, pp. 165–172, 2012.
- [21] I. Orović, V. Papić, C. Ioana, X. Li, and S. Stanković, "Compressive sensing in signal processing: Algorithms and transform domain formulations," *Math. Probl. Eng.*, vol. 2016, 2016, Art. no. 7616393.

- [22] Z. Zhang and B. D. Rao, "Extension of SBL algorithms for the recovery of block sparse signals with intra-block correlation," *IEEE Trans. Signal Process.*, vol. 61, no. 8, pp. 2009–2015, Apr. 2013.
- [23] H. B. Mann and D. R. Whitney, "On a test of whether one of two random variables is stochastically larger than the other," *Ann. Math. Statist.*, vol. 18, no. 1, pp. 50–60, 1947.
- [24] S. S. Shapiro and M. B. Wilk, "An analysis of variance test for normality (complete samples)," *Biometrika*, vol. 52, no. 3/4, pp. 591–611, 1965.
- [25] C. J. Stam, G. Nolte, and A. Daffertshofer, "Phase lag index: Assessment of functional connectivity from multi channel EEG and MEG with diminished bias from common sources," *Human Brain Mapping*, vol. 28, no. 11, pp. 1178–1193, 2007.
- [26] S. S. Poil, W. de Haan, W. M. van der Flier, H. D. Mansvelder, P. Scheltens, and K. Linkenkaer-Hansen, "Integrative EEG biomarkers predict progression to Alzheimer's disease at the MCI stage," *Front Aging Neurosci.*, vol. 5, 2013, Art. no. 58.
- [27] A. Alberdi, A. Aztiria, and A. Basarab, "On the early diagnosis of Alzheimer's disease from multimodal signals: A survey," *Artif. Intell. Med.*, vol. 71, pp. 1–29, 2016.
- [28] E. Capecci, F. C. Morabito, M. Campolo, N. Mammone, D. Labate, and N. Kasabov, "A feasibility study of using the NeuCube spiking neural network architecture for modelling Alzheimer's disease EEG data," in *Advances in Neural Networks: Computational and Theoretical Issues*. New York, NY, USA: Springer, 2015, pp. 159–172.
- [29] E. Capecci, Z. G. Doborjeh, N. Mammone, F. La Foresta, F. C. Morabito, and N. Kasabov, "Longitudinal study of Alzheimer's disease degeneration through EEG data analysis with a NeuCube spiking neural network model," in *Proc. Int. Joint Conf. Neural Netw.*, 2016, pp. 1360–1366.
- [30] C. Bandt and B. Pompe, "Permutation entropy: A natural complexity measure for time series," *Phys. Rev. Lett.*, vol. 88, no. 17, 2002, Art. no. 174102.



Nadia Mammone (M'05) received the Ph.D. degree from the DICEAM Department, Mediterranean University of Reggio Calabria, Reggio Calabria, Italy, 2007.

She is currently the Principal Investigator, with the IRCCS Centro Neurolesi Bonino Pulejo, Messina, Italy, of a research project funded by the Italian Ministry of Health. Formerly, she was a Postdoc Fellow with the DICEAM Department, Mediterranean University of Reggio Calabria. She was an Adjunct Professor of *Neural Networks and Fuzzy Systems* with the Mediterranean University of Reggio Calabria, of *Electronics and Instrumentation* with the Neurophysiopathology Laboratory, and of *Biomedical Signal Processing* with the University of Catanzaro, Italy. She was a Visiting Ph.D. Fellow with the Computational NeuroEngineering Laboratory, University of Florida, Gainesville, FL, USA, and a Visiting Postdoc Fellow with the Communication and Signal Processing Research Group, Imperial College London, London, U.K. Her research interests include biomedical signal processing, neural and adaptive systems, chaos theory, and information theory.

Dr. Mammone was the recipient of the Caianiello Prize from the Italian Neural Networks Society (SIREN) for her Ph.D. dissertation.



Simona De Salvo received the Bachelor's degree in techniques of neurophysiopathology and Master's degree in sciences for health professions in diagnostic techniques from the University of Messina, Messina, Italy, in 2008 and 2011, respectively.

She is currently a Research Fellow with the IRCCS Centro Neurolesi Bonino Pulejo, Messina, Italy.



Lilla Bonanno received the degree in mathematics from the University of Messina, Messina, Italy, in 2007, two second-level Master's degrees in open source and information security from the University of Messina, in 2008 and in advanced methods of neuroimaging from the University of Messina, in 2015, and the Ph.D. degree in neurobiological and clinical sciences from the University of Messina, in 2012.

During her studies in mathematics, she developed an interest in the implementation of algorithms for thyroid tumors segmentation. During her Ph.D., she continued to work on the development of algorithms and to gain expertise on magnetic resonance imaging. Since 2012, she has been a Research Fellow with the IRCCS Centro Neurolesi Bonino Pulejo, Messina, Italy. Her research interests include the clinical application of magnetic resonance functional and diffusion tensor imaging to neurological diseases.

Dr. Bonanno was the recipient of award for her contribution in the field of *Neuroimaging* in 2017 by the Italian Neurological Society.



Cosimo Ieracitano received the Master's degree (*summa cum laude*) in electronic engineering from the Mediterranean University of Reggio Calabria, Reggio Calabria, Italy, in 2013.

He was an Erasmus Student with iniLabs, Institute of Neuroinformatics, ETH Zurich, Zurich, Switzerland, where he carried out his master thesis. After a short industrial experience, he joined the Neurolab's Group, DICEAM Department, Mediterranean University of Reggio Calabria, where he is currently a Ph.D. Fellow under the supervision of Prof. F. C. Morabito. He was a Visiting Ph.D. Fellow with the CogBiD Lab, University of Stirling, Stirling, U.K., under the supervision of Prof. A. Hussain. His research interests include machine learning, deep learning, and biomedical signal processing, especially EEG signals analysis of patients affected by neural disorders.



Silvia Marino received the Ph.D. degree in neurobiological and clinical sciences from the Quantitative Neuroimaging Laboratory, University of Siena, Siena, Italy, 2005.

Her research interests are devoted to the clinical and neuroimaging aspects of neurological disorders. She worked at the Movement and Disorders Ambulatory with the IRCCS Centro Neurolesi Bonino Pulejo, Messina, Italy, where she was involved in several research projects on the clinical and pharmacological aspects of several neurodegenerative disorders. During her Ph.D., she continued to focus on the clinical aspects of several neurological disorders, but also developed a special interest and expertise on neurological diseases involving the brain white matter. In the University of Siena, she worked on the clinical application of magnetic resonance spectroscopy and functional magnetic resonance in brain of patients with neurological disorders. Since 2008, she has been leading the Quantitative NeuroBioImaging Laboratory, IRCCS Centro Neurolesi Bonino Pulejo. Her current research focuses on patients with low levels of consciousness (coma, vegetative state, minimally conscious state, locked-in syndrome).



Angela Marra received the Graduate degree in medicine from the University of Messina, Messina, Italy, in 1991, and her first-level Master's degree in neurology and emergency psychiatry from the University of Messina in 1992.

From 1992 to 1995, she specialized in neurophysiopathology with the University of Messina. From 1996 to 1999, she was with the Policlinico Universitario Messina, Messina, Italy. Since 2000, she has been the Medical Director in neurology with the IRCCS Centro Neurolesi Bonino

Pulejo, Messina, Italy. Since 2004, she has been researching on dementia.



Alessia Bramanti received her Master's degree in electronic engineering from the University of Messina, Messina, Italy, in 2006 and her Ph.D. degree in advanced technologies for the optoelectronics and photonics and electromagnetic modelling from the University of Messina, Messina, Italy, in 2012.

She has many years of proven experience in the analysis, design, development, and evolution of systems and innovative solutions in the healthcare ICT field, advanced computer systems

(grid and cloud technology) for epidemiological database, RFID technology and its application in the clinical field, analysis and processing of electrophysiological signals and neuroradiological images. She is a member of the Italian Telemedicine Society and has been collaborating with the IRCCS Centro Neurolesi Bonino Pulejo, Messina, Italy. She is currently a Research Fellow with the Institute of Applied Sciences and Intelligent Systems "Eduardo Caianiello," National Research Council, Messina, Italy. She is the author of several publications and patents related to methods of data collection via special sensors placed on patients with neurological disease and the transmission of such data via remote monitoring systems.



Francesco C. Morabito (SM'00) received his Degree in electronic engineering from the University of Naples Federico II, Naples (Italy) in 1985. He is a Full Professor of electrical engineering with the Mediterranean University of Reggio Calabria, Reggio Calabria, Italy, where he is also the Vice-Rector for International and Institutional Relations. He has authored more than 400 papers published in international journals/conference proceedings in various fields of engineering. He is the coauthor of 15 books and

holds three international patents. He was a Foreign Member of the Royal Academy of Doctors, Spain (2004) and Member of the Institute of Spain, Barcelona Economic Network (2017). He was the Governor of the International Neural Network Society for 12 years and the President of the Italian Network Society from 2008 to 2014.

Mr. Morabito is a member of the editorial boards of various relevant international journals, including the *International Journal of Neural Systems*, *Neural Networks*, *International Journal of Information Acquisition*, and *Renewable Energy*.